# Improved Design of Special Boundary Elements for T-Shaped Reinforced Concrete Walls

Xiaodong Ji, Dan Liu, Jiaru Qian

*Department of Civil Engineering, Key Laboratory of Civil Engineering Safety and Durability of China Education Ministry, Tsinghua University, Beijing 100084, China.*

**Abstract**: This study examines the design provisions of the Chinese GB 50011-2010 code for seismic design of buildings for the special boundary elements of T-shaped reinforced concrete walls and proposes an improved design method. Comparison of the design provisions of the GB 50011-2010 code and those of the American code ACI 318-14 indicates a possible deficiency in the T-shaped wall design provisions in GB 50011-2010. A case study of a typical T-shaped wall designed in accordance with GB 50011-2010 also indicates the insufficient extent of the boundary element at the non-flange end and overly conservative design of the flange end boundary element. Improved designs for special boundary elements of T-shaped walls are developed using a displacement-based method. The proposed design formulas produce a longer boundary element at the non-flange end and a shorter boundary element at the flange end, relative to those of the GB 50011-2010 provisions. Extensive numerical analysis indicates that T-shaped walls designed using the proposed formulas develop inelastic drift of 0.01 for both cases of the flange in compression and in tension.

**Keywords**: code comparison, displacement-based method, seismic design; special boundary element; T-shaped wall

## 1. Introduction

Reinforced concrete (RC) shear walls are widely used as lateral force-resistant components in high-rise buildings because they provide high lateral stiffness and strength. When subjected to severe ground motion, RC walls are expected to form plastic hinges at the wall base, which then dissipate the seismic energy and reduce the dynamic response of the entire structure accordingly (Moehle et al., 2011). To ensure sufficient inelastic deformation capacity, wall boundary elements that are strengthened using longitudinal and transverse reinforcement are needed for the critical region (i.e., the plastic hinge region) of RC walls.

Special boundary elements with closely spaced transverse reinforcement that are used to confine the concrete and to postpone buckling of the longitudinal rebars are placed where combined seismic and gravity loading would result in high compressive strain demand. The special boundary element must be provided over a wall depth at which the compressive strains exceed the compressive strain capacity of the unconfined concrete, which is typically 0.003 or 0.0033. The ACI 318-14 code provisions specify simplified formulas to determine the extent of the special boundary element based on the flexural compressive depth for both rectangular and flanged wall sections. The Chinese code for seismic design of buildings, GB 50011-2010, provides a specific table to determine the extent of the special boundary element based on the ductility demand and the axial force ratio of the wall. This table has been calibrated via an extensive analysis of rectangular-shaped RC walls (Liang, 2007), but it lacks a thorough validation for T-shaped RC walls. There is therefore a clear need to examine the GB 50011-2010 provisions for the special boundary elements of T-shaped walls.

Over the past two decades, a number of experimental tests have been performed to examine seismic behavior and to validate the design provisions of the New Zealand code and of ACI 318 for T-shaped RC walls (e.g., Goodsir, 1985; Choi et al., 2004; Thomson and Wallace, 2004; Brueggen, 2009). These tests have indicated that the free end of the wall web is prone to premature failure in crushing of concrete and buckling of the longitudinal rebars if the boundary element at the non-flange end is insufficient. The non-flange end of T-shaped walls should thus be provided with a longer boundary element relative to rectangular walls.

The objective of this paper is to examine the GB 50011-2010 design provisions for T-shaped RC walls, and to develop an improved design for such T-shaped walls using a displacement-based method. T-shaped walls may be subjected to multi-directional loading throughout the duration of an earthquake motion (Brueggen, 2009), but this paper focuses on the performance of T-shaped walls when subjected to lateral loading parallel to the wall web. The second section compares the design provisions for special boundary elements of T-shaped walls in ACI 318-14 with those in GB 50011-2010. In the third section, the behavior of typical T-shaped walls that have been designed to meet the ACI 318-14 and GB 50011-2010 provisions is examined via numerical analysis. The fourth section proposes an improved design for the boundary elements of T-shaped RC walls, which aims to update the current GB 50011-2010 provisions. Finally, an extensive analysis is performed to validate the reliability of the proposed T-shaped wall design.

## 2. Comparison of T-shaped Wall Design between US and Chinese Codes

Two important issues are considered in the design of special boundary elements for RC walls: the extent of the boundary elements and the required amount of boundary transverse reinforcement. The following compares the provisions on these two issues specified by ACI 318-14 and GB 50011-2010.

### 2.1 Extent of special boundary elements

The ACI 318-14 provisions use a displacement-based method to determine whether special boundary elements are required for RC walls (Moehle, 2014). The structural system is analyzed to determine the top-level displacement $\delta_u$ under design basis earthquake (DBE) motion and the corresponding maximum value of the wall axial force $N$. Special boundary elements are required for RC walls if

$$c \geq \frac{h}{900\left(\delta_u / H\right)} \tag{1}$$

where $c$ denotes the flexural compression depth corresponding to the nominal moment strength under axial force $N$; $h$ denotes the depth of the wall section; and $H$ denotes the wall height.

When a special boundary element is required, the ACI 318-14 provisions require it to extend horizontally from the wall edge by a distance $l_c$, which is given by:

$$l_c = \max(c - 0.1h, c/2) \tag{2}$$

The ACI 318-14 provisions also specify for T-shaped walls that the boundary element at the flange end, if required, must include the effective flange width in compression and must extend at least 305 mm into the web.

The GB 50011-2010 provisions determine whether or not special boundary elements are required, based on the ductility demand and the design axial force ratio $n_d$=$N_d$/$f_{c,d}A$ for RC walls, where $N_d$ denotes the design axial compressive force applied to the wall, $f_{c,d}$ denotes the design value of the axial compressive strength of concrete, and $A$ denotes the cross-sectional area of the wall. The seismic grade is an important design parameter in GB 50011-2010, which reflects the ductility demand on the structural systems and components. Seismic grades ranging from I to IV correspond to a high ductility requirement gradually decreasing to a low ductility requirement. Special boundary elements are required if the design axial force ratio exceeds 0.1 for highly ductile walls (Seismic Grade I, seismic intensity of 9), 0.2 for highly ductile walls (Seismic Grade I, seismic intensities of 6–8), and 0.3 for moderately ductile walls (Seismic Grades II and III). Note that in the calculation of the design axial force ratio, a value of 1.2 is considered for the load factor and a value of 1.4 is considered for the strength reduction factor of concrete (i.e., the ratio of the nominal value of material strength to the design value). In addition, the GB 50011-2010 provisions only include the gravity load effect in the calculation of the axial force ratios of structural walls, while the axial force that is induced by seismic action is excluded.

Table 1 summarizes the extent of the special boundary elements required by the GB 50011-2010 provisions for T-shaped walls. The non-flange end of the wall requires a slightly longer boundary element than the flange end. Increases in the ductility demand and in the axial force ratio lead to an increase in the extent of the special boundary elements.

Table 1. Extents of special boundary elements of T-shaped walls specified in GB 50011-2010

| Location | Grade I (seismic intensity of 9) | | Grade I (seismic intensities of 6 to 8) | | Grades II and III | |
|---|---|---|---|---|---|---|
| | $n_d$≤0.2 | $n_d$>0.2 | $n_d$≤0.3 | $n_d$>0.3 | $n_d$≤0.4 | $n_d$>0.4 |
| Flange end | 0.15$h$ | 0.20$h$ | 0.10$h$ | 0.15$h$ | 0.10$h$ | 0.15$h$ |
| Non-flange end | 0.20$h$ | 0.25$h$ | 0.15$h$ | 0.20$h$ | 0.15$h$ | 0.20$h$ |

Note: $h$ denotes the depth of the wall section, and $n_d$ denotes the design value of the axial force ratio.

To compare the provisions for special boundary elements in the ACI 318-14 and GB 50011-2010 codes, a typical T-shaped wall section is considered for a case study. Figure 1 shows the cross-sectional geometry of the wall. The wall's sectional depth, flange width, web thickness, and flange thickness are 5400, 5200, 400, and 400 mm, respectively. Figure 2 shows the extent of the special boundary elements of the wall when designed as per the two design codes under various axial force ratios. The boundary element at the flange end is not required for this wall by the ACI 318-14 provisions, while it is required by the GB 50011-2010 provisions, as shown in Figure 2(a). Both codes require the boundary elements to be provided at the non-flange end for this wall. Figure 2(b) indicates that when the design axial force ratio exceeds 0.25, the ACI 318-14 provisions require a significantly longer special boundary element at the non-flange end than the GB 50011-2010 provisions. Code comparison (Liu 2014) also shows that Eurocode 8 requires a much longer boundary element at the non-flange end than GB 50011-2010 for highly ductile T-shaped walls, which indicates a possible deficiency in the T-shaped wall design provisions of GB 50011-2010.

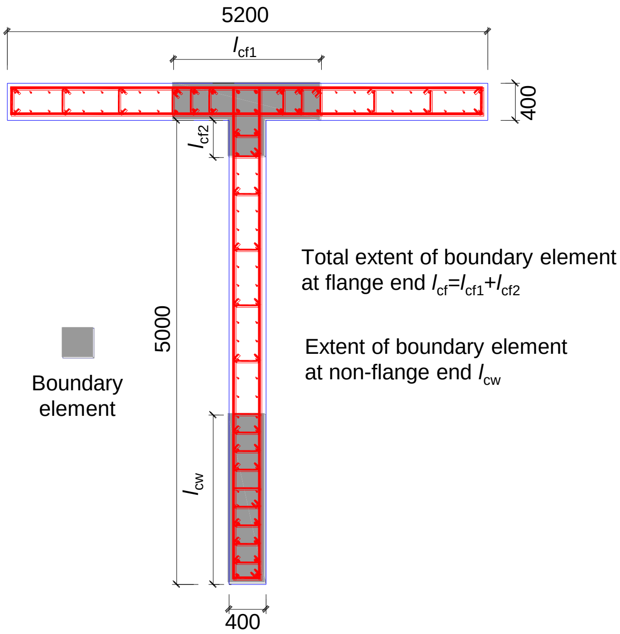


Fig. 1. T-shaped wall section used for case study (units: mm).

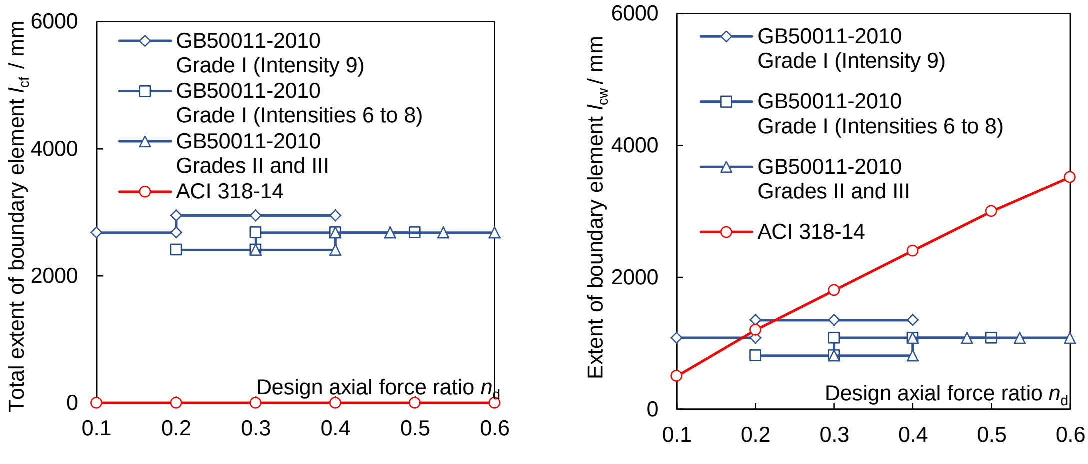


(a) Flange end (b) Non-flange end

Fig. 2. Comparison of the extents of special boundary elements of T-shaped walls.

## 2.2 Amount of boundary transverse reinforcement

A discrepancy exists in the treatment of the transverse reinforcement of the special boundary elements between the ACI 318-14 and GB 50011-2010 code provisions. According to the ACI 318-14 provisions, the entire boundary element region is required to have a uniform level of transverse reinforcement. In contrast, in the GB 50011-2010 provisions, the boundary element is divided into two regions, as shown in Figure 3. Region I is intended to have double the amount of transverse reinforcement used in Region II as higher compressive strains are expected to develop in Region I under the combined axial compression and bending moment.

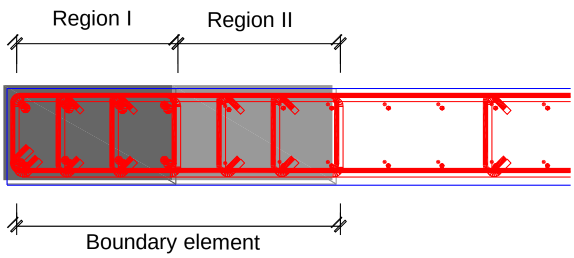


Fig. 3. Special boundary elements of T-shaped walls.

Based on the ACI 318-14 provisions, the amount of boundary transverse reinforcement must satisfy the following equations:

$$A_{shy} \geq 0.09 \frac{s b_c f_c^{'}}{f_{yv}} \tag{3-a}$$

$$A_{shx} \geq 0.09 \frac{s h_c f_c^{'}}{f_{yv}} \tag{3-b}$$

where $A_{shx}$ and $A_{shy}$ denote the cross-sectional areas of the boundary transverse rebars in the $x$ and $y$ directions, respectively, at a vertical spacing $s$ (see Figure 4); $b_c$ and $h_c$ denote the width and the depth of the confined core concrete, respectively (see Figure 4); $f_{yv}$ denotes the yield strength of the transverse rebars; and $f_c^{'}$ denotes the cylinder compressive strength of the concrete.

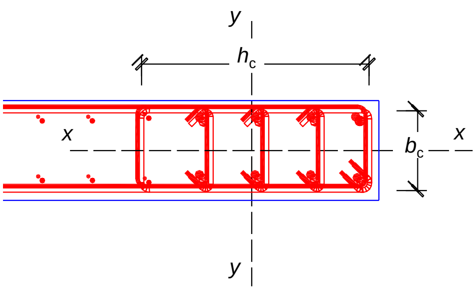


Fig. 4. Boundary transverse reinforcement required by ACI 318-14.

In GB 50011-2010, the amount of transverse reinforcement required is expressed in terms of the stirrup characteristic value $\lambda_v$ (known as the mechanical volumetric ratio in Eurocode 8), which is given by:

$$\lambda_v = \rho_s f_{yv} / f_c \tag{4}$$

where $\rho_s$ denotes the volumetric transverse reinforcement ratio (i.e., the ratio of the volume of the transverse reinforcement over that of the concrete core confined by that transverse reinforcement), $f_{yv}$ denotes the yield strength of the transverse reinforcement, and $f_c$ denotes the axial compressive strength of the concrete.

The amount of boundary transverse reinforcement required is determined based on the ductility demand and the design axial force ratio according to the GB 50011-2010 provisions. Figure 5 shows the stirrup characteristic value $\lambda_v$ at Region I of the boundary element required by the GB 50011-2010 provisions, and compares it with the equivalent value of the boundary transverse reinforcement required by the ACI 318-14 provisions. For comparison, the design values of material strength specified in GB 50010-2010 are used in the calculations of both the axial force ratio and the stirrup characteristic value. Figure 5 indicates that the amount of boundary transverse reinforcement required by the ACI 318-14 provisions is more than 37% higher than that required by the GB50011-2010 provisions.

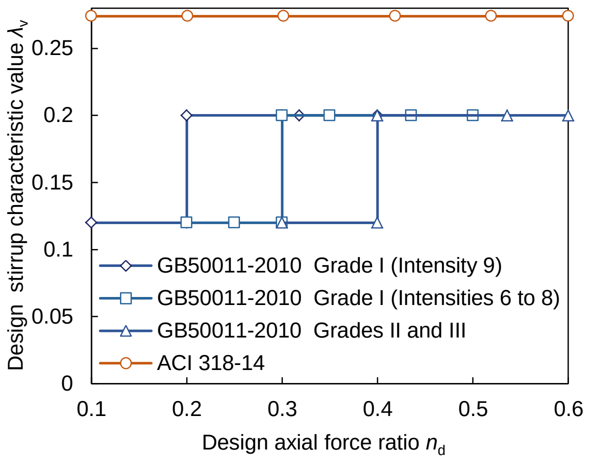


Fig. 5. Comparison of required amounts of boundary transverse reinforcement.

## 3. Performance Comparison of T-shaped Walls: Case Study

### 3.1 Design of T-shaped walls for case study

A case study is performed to compare the performance of T-shaped walls that were designed according to the GB 50011-2010 provisions with those designed according to the ACI 318-14 provisions. A typical T-shaped wall with a cross-section of the type shown in Figure 1 is used in this case study. This cantilever wall has an aspect ratio (i.e., a height-to-width ratio) of 3. The design axial compressive force and the shear force applied at the top of the cantilever wall are 36000 and 3670 kN, respectively, and result in a bending moment of 55000 kN·m being developed at the wall base. The concrete used in the wall has a strength grade of C45 (nominal axial compressive strength $f_{ck}$ = 29.6 MPa and design axial compressive strength $f_{c,d}$ = 21.2 MPa). The longitudinal boundary rebars have a strength grade of HRB400 (nominal yield strength $f_y$ = 400 MPa and design yield strength $f_{yd}$ = 360 MPa), and the other rebars have a strength grade of

HRB335 (nominal yield strength $f_y$ = 335 MPa and design yield strength $f_{yd}$ = 300 MPa). The design axial force ratio of the wall is 0.5.

Two T-shaped walls are designed as a Grade I wall (seismic intensity of 8) according to the GB 50011-2010 provisions and as a special structural wall using the ACI 318-14 provisions, and are referred to as $TW_{GB}$ and $TW_{ACI}$, respectively. Figure 6 shows the sectional geometries and the reinforcement details of these two walls. The special boundary element at the non-flange end of $TW_{ACI}$ is very long, and has a length of approximately 0.55 times the wall's sectional depth, while that of $TW_{GB}$ is only 0.2 times the sectional depth. In contrast, the special boundary element at the flange end is not provided for $TW_{ACI}$ according to the ACI 318-14 provisions, while $TW_{GB}$ has a boundary element at the flange–web intersection, as required by the GB 50011-2010 provisions. The total cross-sectional area of the boundary elements at the two ends of $TW_{GB}$ is 23% larger than the corresponding area of $TW_{ACI}$.

The two walls have similar levels of distributed reinforcement and longitudinal boundary reinforcement. The stirrup characteristic value of the boundary transverse reinforcement of $TW_{ACI}$ is 0.3, while the values of $TW_{GB}$ in Region I and Region II are 0.27 and 0.13, respectively. The total amount of boundary transverse reinforcement of $TW_{ACI}$ is 30% higher than that of $TW_{GB}$.

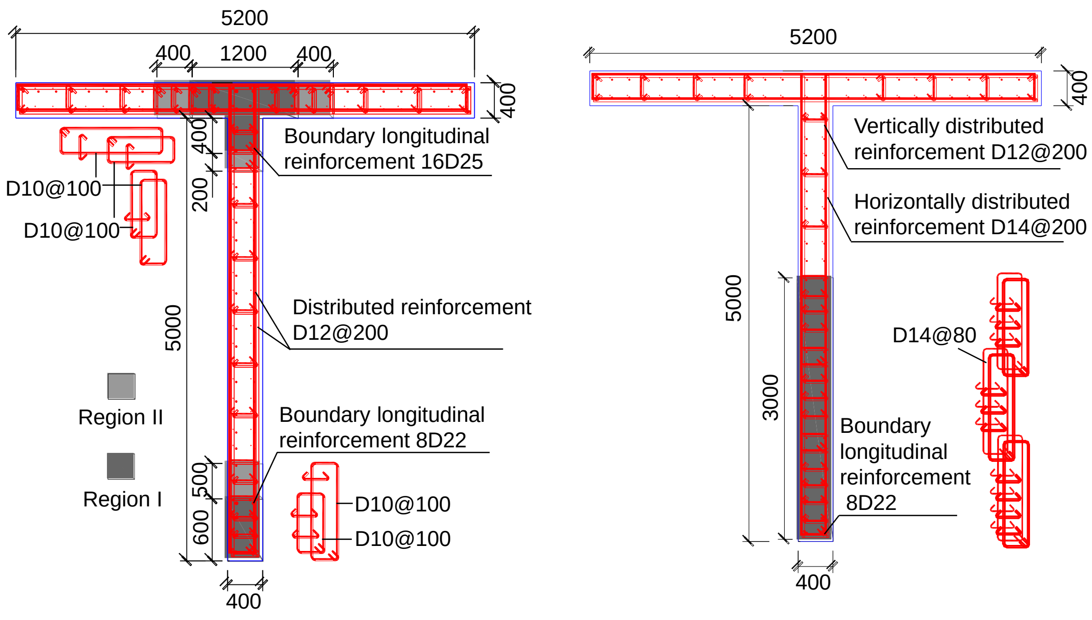


(a) $TW_{GB}$ (b) $TW_{ACI}$

Fig. 6. T-shaped wall sections designed according to the (a) Chinese and (b) US codes (units: mm).

### 3.2 Analysis model

Cross-sectional analysis of the T-shaped wall is performed using Xtract software, which assumes that a plane section remains plane after bending. A model that was developed by Mander et al. (1988) is used to represent the uniaxial strain-stress relationship of the concrete in compression. This model can reflect the effects of the confinement provided by the transverse reinforcement. Figure 7(a) shows the strain-stress relationships of the concrete at the various regions of the walls. The tensile strain-stress relationship of the concrete is simplified as a bilinear curve (see Figure 7(a)), where $f_t$ denotes the axial tensile strength of the concrete, $E_c$ denotes the Young's modulus of the concrete, and the ultimate tensile strain $\varepsilon_{tu}$ is assumed to be $2f_t/E_c$. A bilinear model, as shown in Figure 7(b), is then adopted to represent the strain-stress relationships of the rebars, where the hardening modulus is assumed to be 1% of the Young's modulus of the steel. The nominal material strength values specified in the GB 50010-2010 code are used in this analysis.

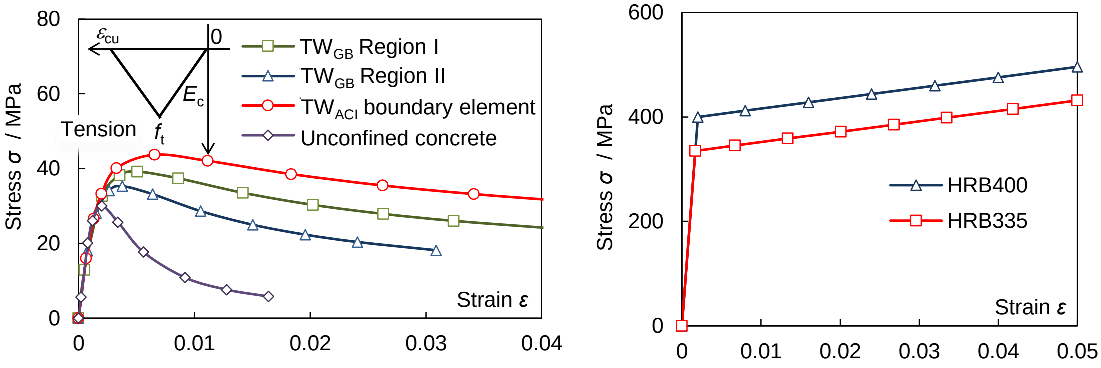


(a) Concrete (b) Steel

Fig. 7. Uniaxial stress-strain relationship curves of the wall materials.

After the moment-curvature relations of the wall sections are calculated in the cross-sectional analysis, the lateral displacement of a flexural-dominated cantilever wall can then be obtained by integrating the curvature up the height of the wall. After the wall yields fully at its base, a plastic hinge model is used to provide an approximate assessment of the wall's lateral drift. This model assumes that the plastic deformation of the wall is concentrated at the plastic hinge of the wall base, as shown in Figure 8(a). The plastic curvature is assumed to be uniformly distributed along the plastic hinge, and the plastic hinge length $l_p$ is assumed to be half of the wall's sectional depth (Thomsen and Wallace, 2004). Therefore, the lateral deformation $\varDelta$ at the top of the wall is calculated as follows:

$$\varDelta = \frac{1}{3}H^2\phi \qquad \text{(for } M<M_y\text{)} \qquad (5a)$$

$$\varDelta = \frac{1}{3}\phi_y H^2 + (\phi - \phi_y) l_p H \qquad \text{(for } M\geq M_y\text{)} \qquad (5b)$$

where $\phi$ denotes the curvature of the wall's base section, $H$ denotes the height of the cantilever wall, $\phi_y$ denotes the yield curvature of the wall section, $M$ denotes the bending moment at the wall base, and $M_y$ denotes the yielding flexural strength of the wall section. Using these equations, the lateral force-displacement relationship of a cantilever wall can be obtained from the sectional moment-curvature relationship estimated from the Xtract analysis. The $P$-$\varDelta$ effect can be included with the wall base moment, which is calculated as $M = FH + N\varDelta$, where $F$ and $N$ are the lateral and axial compressive forces, respectively.

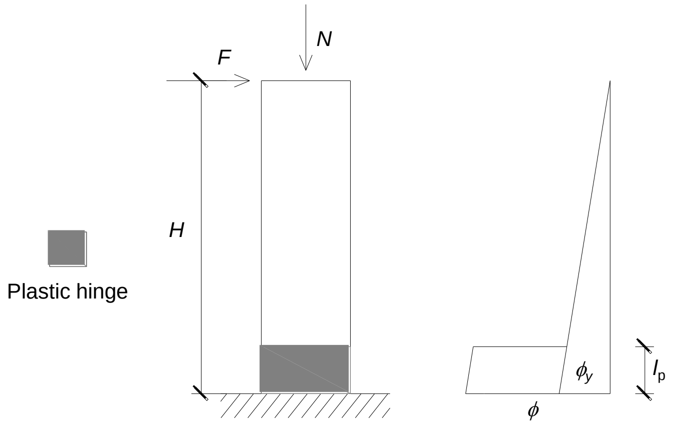


Fig. 8. Plastic hinge model of cantilever wall.

Four T-shaped RC cantilever wall specimens that were tested in previous studies are used to validate the numerical model. Table 2 summarizes the major design parameters of these wall specimens. The shear-to-span ratios of these cantilever wall specimens varied from 1.75 to 3, and their design axial force ratios varied from 0.17 to 0.29. All specimens failed in a flexural mode. Figure 9 shows the lateral force versus displacement relationships of the specimens that were obtained from the numerical model compared with the corresponding test results. These T-shaped wall specimens all showed unsymmetrical hysteretic responses, with higher stiffness and strength values and lower ductility in the flange-in-tension loading direction. While the numerical analysis overestimates the stiffnesses of the wall specimens because it neglects the wall's shear deformation, it generally captures the strength and deformation characteristics of these wall specimens correctly.

Table 2. Design parameters of T-shaped wall specimens.

| Specimen no. | $b_f \times t_f$ / m | $h \times t_w$ / m | $n_d$ | $l_{cw}$ / $h$ | Shear-to-span ratio |
|---|---|---|---|---|---|
| T800-2 in Li (2011) | 0.8 × 0.1 | 0.8 × 0.1 | 0.29 | 0.14 | 1.75 |
| SDT800-05 in Zhang and Li (2013) | 0.8 × 0.1 | 0.8 × 0.1 | 0.17 | 0.14 | 1.75 |
| TW1 in Thomsen and Wallace (2004) | 1.2 × 0.1 | 1.2 × 0.1 | 0.20 | 0.14 | 3 |
| TW2 in Thomsen and Wallace (2004) | 1.2 × 0.1 | 1.2 × 0.1 | 0.20 | 0.36 | 3 |

Note: $b_f$ denotes flange width; $t_f$ denotes flange thickness; $h$ denotes depth of the wall cross-section; $t_w$ denotes web thickness; and $l_{cw}$ denotes the extent of the boundary element at the non-flange end.

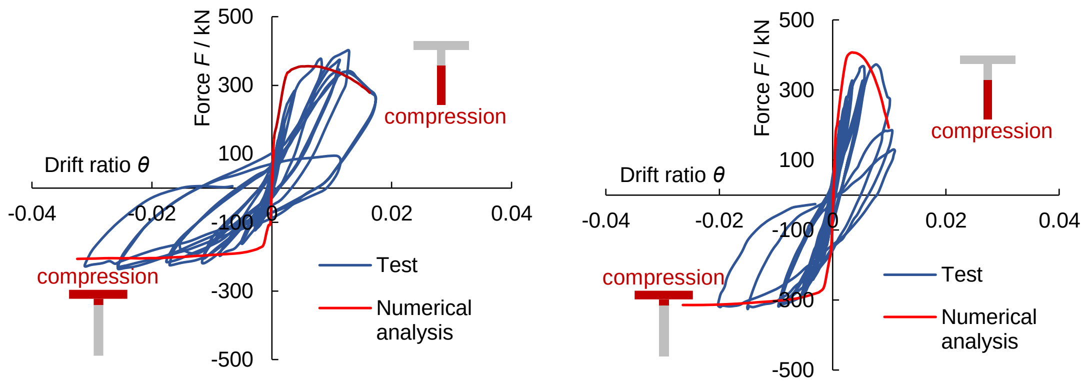


(a) T800-2 in Li (2011) (b) SDT800-05 in Zhang and Li (2013)

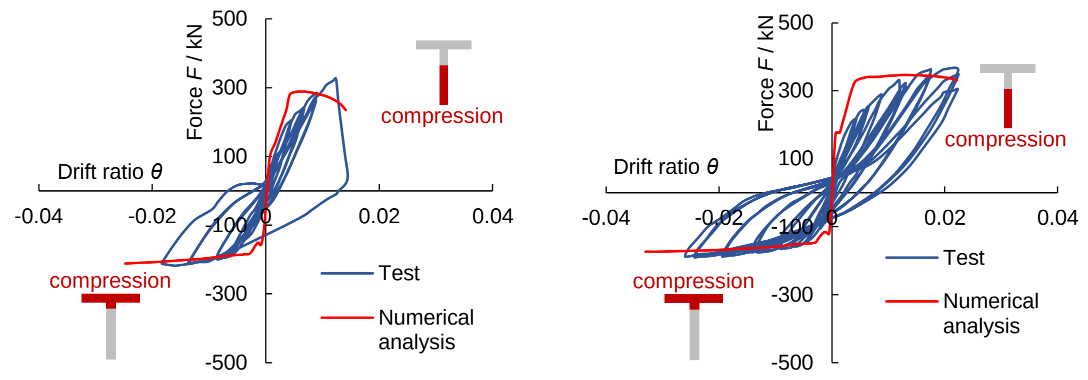


(c) TW1 in Thomsen and Wallace (2004) (d) TW2 in Thomsen and Wallace (2004)

Fig. 9. Analysis results of experimental specimens.

### 3.3 Performance of T-shaped walls

Figure 10 shows the lateral force versus displacement relationship of $TW_{GB}$ and $TW_{ACI}$, as estimated by numerical analysis. The results indicate that, for the flange-in-compression loading direction, the lateral force versus displacement curves of the two walls are quite similar. This is consistent with the test observation by Thomsen and Wallace (2004), where two T-shaped wall specimens showed very similar behavior for the flange-in-compression loading direction, despite the fact that they had different boundary elements at the non-flange end. Both $TW_{GB}$ and $TW_{ACI}$ develop significantly high inelastic drift of approximately 0.03. At this drift of 0.03, the compressive zone depth is a small fraction of the total depth of the wall and the compressive strain at the flange end is 0.002, which is lower than the compressive strain capacity of unconfined concrete. Therefore, provision of special confinement reinforcement at the flange end is likely to be unnecessary for these walls. A recent test by Lu et al. (2015) also indicates that this conclusion is likely; in the test, the T-shaped wall specimen had a flange-to-web area ratio (i.e., the ratio of the cross-sectional area of the flange to that of the web) and an axial force ratio that were similar to those of $TW_{GB}$ and $TW_{ACI}$, although the specimen included steel profiles that were embedded in the wall boundary.

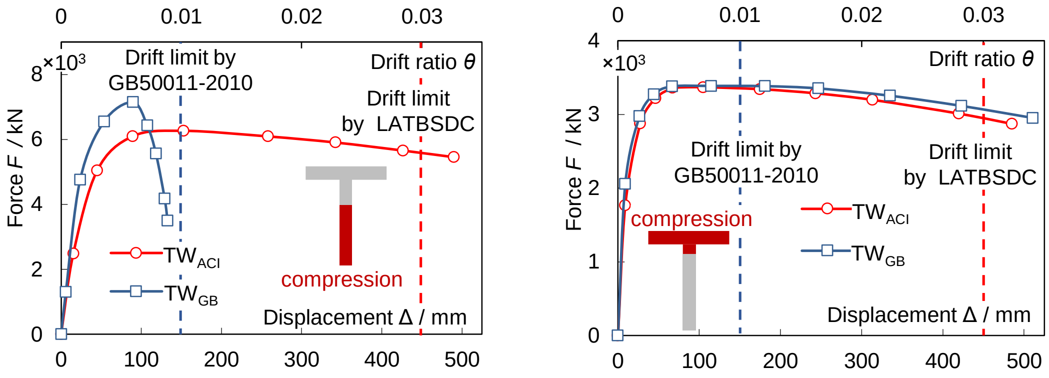


(a) Non-flange end in compression (b) Flange end in compression

Fig. 10. Lateral force-displacement relationship curves of T-shaped walls.

For the flange in tension, $TW_{GB}$ shows much more rapid degradation of post-peak load strength than $TW_{ACI}$. $TW_{GB}$ corresponds to an ultimate drift of 0.008, which is defined as the post-peak drift at the instant when the lateral load decreases to 85% of its peak value. The inelastic drift ratio capacity of $TW_{GB}$ is lower than the value of 0.01 required in the GB 50011-2010 code provision. At the drift of 0.008, the unconfined web concrete beyond the boundary element developed a large compressive strain of 0.006, which significantly exceeds the value of 0.0033. This premature failure caused by crushing of the web concrete indicates the inadequate extent of the special boundary element at the non-flange end of $TW_{GB}$. $TW_{ACI}$ successfully developed inelastic drift of 0.03. At the drift of 0.03, the boundary element at the non-flange end of $TW_{ACI}$ is over the region where the compressive strains exceed 0.0033.

This case study demonstrates that the provisions of GB 50011-2010 for T-shaped walls might actually provide an inadequate boundary element at the non-flange end and an overly conservative boundary element at the flange end of these walls. Special boundary elements designed per the ACI 318-14 provisions appear to be appropriate to ensure the high inelastic drift capacity of the T-shaped walls. However, it should be noted that GB 50011-2010 requires an inelastic drift ratio capacity of 0.01 for RC walls, while US codes generally require much higher inelastic drift ratio capacity. For example, the LATBSDC (2008) requires an inelastic drift ratio capacity of 0.03 for RC wall structures. The formulas of the ACI 318-14 code may then lead to overly conservative design of the boundary element at the non-flange end for T-shaped walls with a design inelastic drift of 0.01.

## 4. Improved T-shaped Wall Design

Wallace (1994) proposed a displacement-based design method for RC walls, which then formed the basis of the ACI 318-14 design provisions for RC walls. In this section, this displacement-based method is extended for T-shaped walls with a target deformation capacity that is in line with the GB 50011-2010 provisions. Based on this method, simplified formulas that can be used to determine the extent of the boundary elements of T-shaped walls will be proposed to update the existing GB 50011-2010 provisions. For displacement-based design, the strain distribution in each section is assumed to satisfy the condition that the plane sections remain plane after bending, and the use of this assumption was found to be appropriate for the analysis of flexural-dominated T-shaped walls (Thomson and Wallace, 2004).

### 4.1 Extent of special boundary element at the non-flange end

At the target drift, the special boundary element should be provided over a wall depth where the compressive strains exceed a limiting value of 0.0033 (see Figure 11). Therefore, the extent of the special boundary element $l_c$ is given by:

$$l_c = c - 0.0033/\phi \tag{6}$$

where $c$ denotes the flexural compressive depth of the wall at the design drift, and $\phi$ denotes the wall base section curvature at the design drift.

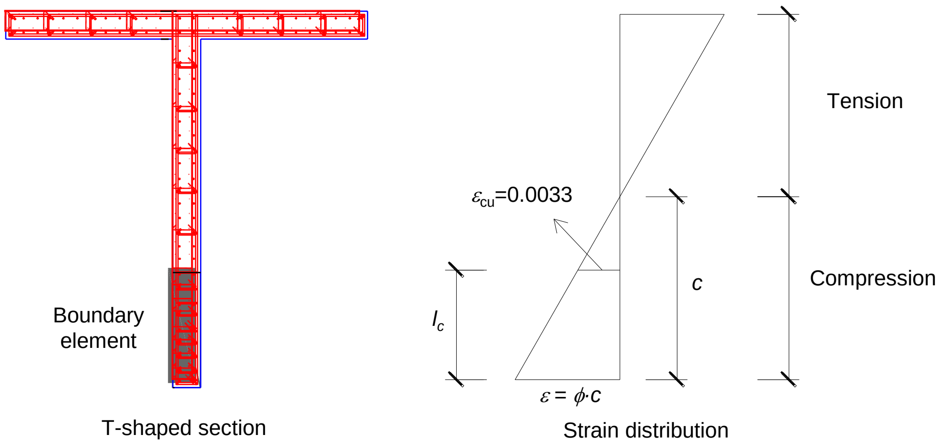


Fig. 11. Calculation of the extent of boundary element at the non-flange end for T-shaped walls.

The test results of Thomson and Wallace (2004) indicated that the flexural compression depth $c$ of a T-shaped wall shows little variation after boundary longitudinal reinforcement yielding occurs. Therefore, the value of $c$ at the drift of 0.01 is approximately equal to the value corresponding to the wall's moment strength under axial force $N$, which is approximately equivalent to Eq. (7). The equation neglects the influence of the unbalanced axial forces of the longitudinal rebars at both ends. This unbalanced force is found to be negligible relative to the applied axial load for most T-shaped walls with axial force ratios of more than 0.1.

$$c = \frac{N}{\alpha\beta f_{cc} t_w} \tag{7}$$

where $N$ denotes the axial compressive force applied to the wall, $f_{cc}$ denotes the axial compressive strength of the confined concrete, $\alpha$ and $\beta$ are equivalent stress block parameters, and $t_w$ denotes the web thickness. The actual axial compressive force applied to the wall is calculated using:

$$N = \frac{n_d f_{c,d} A}{\gamma_G} \tag{8}$$

where $n_d$ is the design axial force ratio, $f_{c,d}$ is the design value of the axial compressive strength of concrete, $A$ denotes the gross cross-sectional area of the T-shaped wall, and $\gamma_G$ =1.2 denotes the load factor for gravity.

The curvature of the wall base section $\phi$ can be estimated from the rotation of the wall's plastic hinge by assuming that the curvature is distributed uniformly along the plastic hinge, and is given by:

$$\phi = \theta_{\mathrm{p}} / l_{\mathrm{p}} \tag{9}$$

where $\theta_{\mathrm{p}}$ denotes the rotation of the plastic hinge and $l_{\mathrm{p}}$ denotes the plastic hinge length. Because a large volume of the test data that was collected in FEMA P-58 indicates that the rotation of the plastic hinges in slender wall specimens is nearly identical to the inelastic drift ratio in each case, the value of $\theta_{\mathrm{p}}$ is thus used as the design inelastic drift of these walls, i.e., 0.01. Note that the plastic hinge length is taken to be half of the depth of the wall section $h$.

Substitution of Eqs.(7) to (9) into Eq.(6) yields

$$l_{\mathrm{c}} = \frac{1}{\gamma_{\mathrm{G}}} \frac{1}{\alpha\beta} \frac{f_{\mathrm{c,d}}}{f_{\mathrm{cc}}} \frac{n_{\mathrm{d}} A}{t_{\mathrm{w}}} - 0.17h \,. \tag{10}$$

For concrete with strength grades in the range from C30 to C60, which is the range that is commonly used for RC walls, the values of $\alpha\beta$ vary slightly from 0.77 to 0.8. Therefore, a conservatively selected value of 0.77 is used for $\alpha\beta$ in the following analysis.

In accordance with the work of Qian et al. (2002), the axial compressive strength of confined concrete $f_{\mathrm{cc}}$ can be estimated as follows:

$$f_{\mathrm{cc}} = (1 + 1.76\lambda_{\mathrm{v}}) f_{\mathrm{ck}} \tag{11}$$

where $\lambda_{\mathrm{v}}$ denotes the stirrup characteristic value of the boundary transverse reinforcement, and $f_{\mathrm{ck}}$ denotes the nominal value of the axial compressive strength of the unconfined concrete, $f_{\mathrm{ck}} = 1.4 f_{\mathrm{c,d}}$. Therefore, the ratio of $f_{\mathrm{c,d}}/f_{\mathrm{cc}}$ can be calculated as follows:

$$\frac{f_{\mathrm{c,d}}}{f_{\mathrm{cc}}} = \frac{1}{1.4 + 2.46\lambda_{\mathrm{v}}} \tag{12}$$

Because the value of $\lambda_{\mathrm{v}}$ for the special boundary elements of RC walls varies from 0.12 to 0.20 in line with the GB 50011-2010 provisions, the ratio of $f_{\mathrm{c,d}}/f_{\mathrm{cc}}$ varies slightly from 0.59 to 0.53, and a value of 0.60 is thus used in the following analysis for simplicity.

Substitution of the values for $\gamma_{\mathrm{G}}$, $\alpha\beta$ and $f_{\mathrm{c,d}}/f_{\mathrm{cc}}$ into Eq. (10) yields

$$\frac{l_{\mathrm{c}}}{h} = 0.65 \frac{n_{\mathrm{d}} A}{A_{\mathrm{w}}} - 0.17 \tag{13}$$

where $A_{\mathrm{w}} = t_{\mathrm{w}} h$ denotes the cross-sectional area of the wall web. This indicates that the relative extent of the special boundary element at the non-flange end of a T-shaped wall relies on the flange-to-web area ratio and the design axial force ratio. Increases in the flange-to-web area ratio and the axial force ratio lead to increased requirements for the extent of the boundary element.

### 4.2 Extent of special boundary element at flange end

A similar analysis is now applied to the T-shaped walls for the flange-in-compression loading direction. Two cases are taken into account, i.e., where the compression zone is within the flange or is beyond the flange. If Eq. (14) is satisfied, then the compression zone is within the flange; otherwise, the zone extends into the web.

$$c = \frac{N}{\alpha\beta f_{\mathrm{ck}} b_{\mathrm{f}}} = \frac{n_{\mathrm{d}} f_{\mathrm{c,d}} A}{\gamma_{\mathrm{G}} \alpha\beta f_{\mathrm{ck}} b_{\mathrm{f}}} \approx 0.8\frac{n_{\mathrm{d}} A}{b_{\mathrm{f}}} \le t_{\mathrm{f}} \tag{13}$$

where $b_{\mathrm{f}}$ denotes the effective width of the flange, and $t_{\mathrm{f}}$ denotes the flange thickness.

In the former case, the length of the special boundary element $l_{\mathrm{c}}$ is given by:

$$l_{\mathrm{c}} = c - 0.0033/\phi = 0.8\frac{n_{\mathrm{d}} A}{b_{\mathrm{f}}} - 0.17h \tag{14}$$

If $l_{\mathrm{c}}$<0, i.e., if $b_{\mathrm{f}}h/(n_{\mathrm{d}}A)$>4.7, the special transverse reinforcement is not necessarily required to confine the concrete at the flange-web intersection. Otherwise, the entire effective width of the flange will be designed as a special boundary element.

In the latter case, i.e., where the compression zone extends into the web, the flexural compressive depth $c$ is calculated as follows:

$$c = \frac{N - f_{\mathrm{ck}}(b_{\mathrm{f}} - t_{\mathrm{w}})t_{\mathrm{f}}}{\alpha\beta f_{\mathrm{ck}} t_{\mathrm{w}}} = \frac{n_{\mathrm{d}} f_{\mathrm{c,d}} A}{\gamma_{\mathrm{G}} \alpha\beta f_{\mathrm{ck}} t_{\mathrm{w}}} - \frac{1}{\alpha\beta}(\frac{b_{\mathrm{f}}}{t_{\mathrm{w}}} - 1)t_{\mathrm{f}} \approx 0.8\frac{n_{\mathrm{d}} A}{t_{\mathrm{w}}} - 1.3(\frac{b_{\mathrm{f}}}{t_{\mathrm{w}}} - 1)t_{\mathrm{f}} \tag{15}$$

Then, the length of the special boundary element $l_{\mathrm{c}}$ is given by:

$$l_{\mathrm{c}} = c - 0.0033/\phi = 0.8\frac{n_{\mathrm{d}} A}{t_{\mathrm{w}}} - 1.3(\frac{b_{\mathrm{f}}}{t_{\mathrm{w}}} - 1)t_{\mathrm{f}} - 0.17h \tag{16}$$

Figure 12 shows the design procedure for the boundary element at the flange end of a T-shaped wall. It should be noted here that the special boundary elements at the two edges shall at least be over the ordinary boundary element zones that are specified by the GB 50011-2010 provisions.

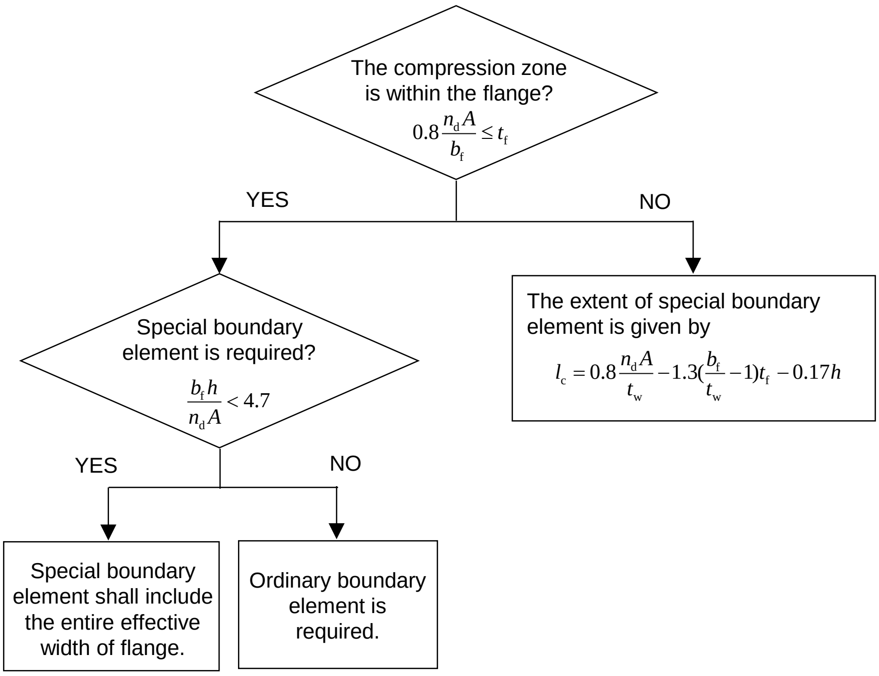


Fig. 12. Design procedure for boundary element at flange end.

## 5. Validation of the Proposed Design Formulas

An extensive analysis is implemented to validate the reliability of the proposed design formulas. A total of 12 numerical T-shaped wall models are considered, where the flange width, the axial force ratio, and the shear-to-span ratio of the wall are all taken as variables. Figure 13 shows the sectional geometry of these walls, and Table 3 summarizes the design parameters. Two cases of flange width are considered: a wide flange of 5.2 m and a moderate flange of 2.4 m. Three design values of the axial force ratio are considered, where 0.2, 0.4, and 0.6 correspond to the low, moderate, and high axial force ratios, respectively. The shear-to-span ratios of the walls are assumed to be 2.5 and 3.5.

The special boundary elements of these walls are designed using the proposed formulas. The transverse reinforcement of boundary elements are designed according to the GB 50011-2010 provisions. Table 3 presents the extents of the boundary elements and Figure 13 shows the reinforcement details of these walls. It should be noted that, with the exception of T2400-2.5-0.6 and T2400-3.5-0.6, special boundary elements are not required at the flange ends of the walls and ordinary boundary elements are therefore provided at the flange-web intersections.

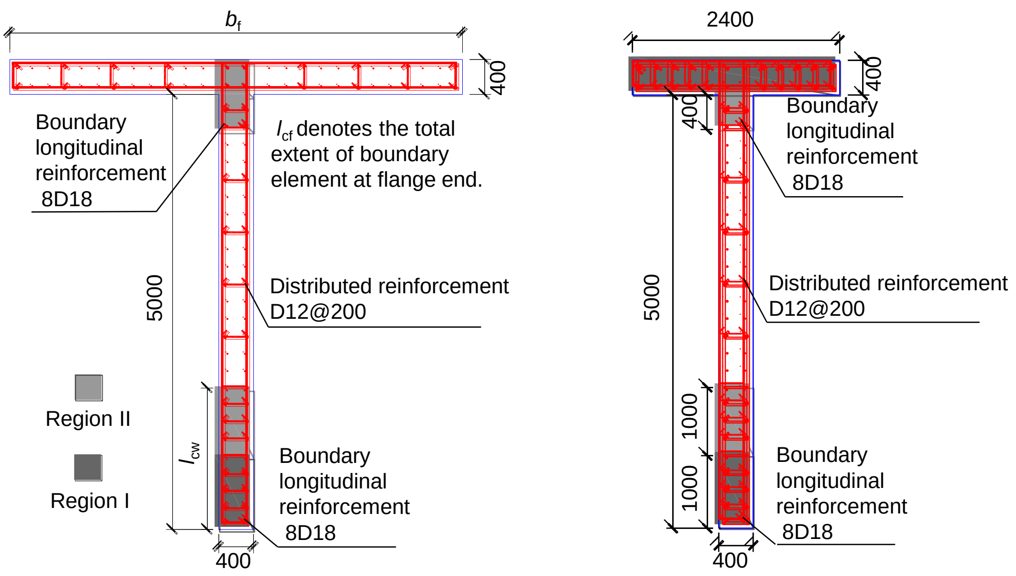


(a) Wall section (except for T2400-2.5-0.6 and T2400-3.5-0.6)

(b) Wall section for T2400-2.5-0.6 and T2400-3.5-0.6

Fig. 13. Sectional geometries and reinforcement details of T-shaped walls (units: mm).

Table 3. Design parameters of T-shaped walls.

| Wall no. | Flange width $b_f$ (m) | Shear-to-span ratio | $n_d$ | Extent of boundary element (m) | | Stirrup characteristic value $\lambda_v$ | |
|---|---|---|---|---|---|---|---|
| | | | | Non-flange end $l_{cw}$ | Flange end $l_{cf}$ | Region I | Region II |
| T2400-2.5-0.2 | | | 0.2 | 0.4 | 0.8 | 0.10 | 0.10 |
| T2400-2.5-0.4 | 2.4 | 2.5 | 0.4 | 1.0 | 0.8 | 0.26 | 0.13 |
| T2400-2.5-0.6 | | | 0.6 | 2.0 | 2.8 | 0.22 | 0.11 |
| T2400-3.5-0.2 | 2.4 | 3.5 | 0.2 | 0.4 | 0.8 | 0.1 | 0.1 |

| | | | | | | |
|---|---|---|---|---|---|---|
| T2400-3.5-0.4 | | | 0.4 | 1.0 | 0.8 | 0.26 | 0.13 |
| T2400-3.5-0.6 | | | 0.6 | 2.0 | 2.8 | 0.22 | 0.11 |
| T5200-2.5-0.2 | | | 0.2 | 0.4 | 0.8 | 0.10 | 0.10 |
| T5200-2.5-0.4 | 5.2 | 2.5 | 0.4 | 1.8 | 0.8 | 0.22 | 0.11 |
| T5200-2.5-0.6 | | | 0.6 | 3.0 | 0.8 | 0.23 | 0.12 |
| T5200-3.5-0.2 | | | 0.2 | 0.4 | 0.8 | 0.10 | 0.10 |
| T5200-3.5-0.4 | 5.2 | 3.5 | 0.4 | 1.8 | 0.8 | 0.22 | 0.11 |
| T5200-3.5-0.6 | | | 0.6 | 3.0 | 0.8 | 0.23 | 0.12 |

Note: For the wall nomenclature, the first number denotes the flange width (units: mm), the second number denotes the shear-to-span ratio, and the third number is the design axial force ratio.

Using the section analysis produced by Xtract and the plastic hinge model described in subsection 3.2, the lateral force-displacement relationship curves of these T-shaped walls can be estimated, as shown in Figure 14. The results indicate that in both cases, where the flange is either in compression or in tension, the ultimate drift ratios of all these walls exceed 0.01, which is the inelastic drift ratio required by the GB 50011-2010 provisions.

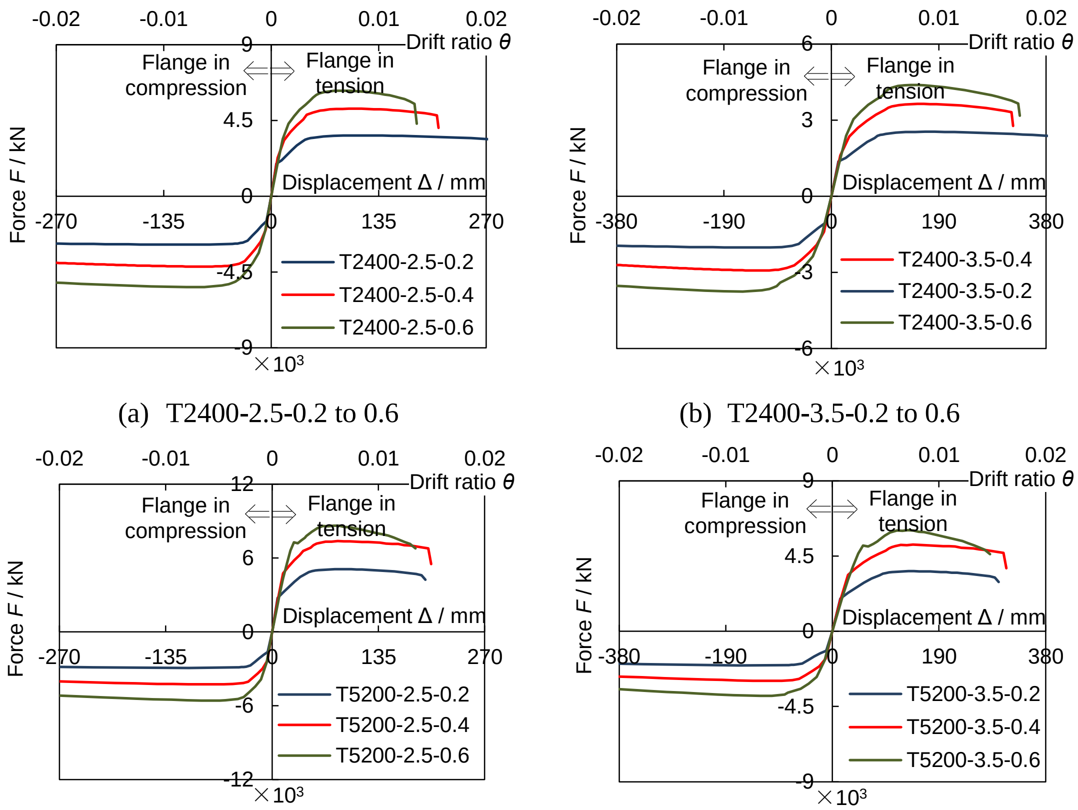


(a) T2400-2.5-0.2 to 0.6 (b) T2400-3.5-0.2 to 0.6

(c) T5200-2.5-0.2 to 0.6 (d) T5200-3.5-0.2 to 0.6

Fig. 14. Lateral force-displacement relationship curves of the T-shaped walls.

Figure 15 compares the extent of the boundary element at the non-flange end of the walls when designed according to the GB 50011-2010 provisions and when using the proposed design formulas. The figure also indicates the locations where the compressive strain exceeds 0.0033 at the base sections of these walls at the drift of 0.01. It is shown that use of the proposed design formulas results in a special boundary element of appropriate extent, while use of the GB 50011-2010 provisions may lead to a boundary element at the non-flange end less than the region where the compressive strain exceeds 0.0033 when the walls are subjected to moderate to high axial force ratios.

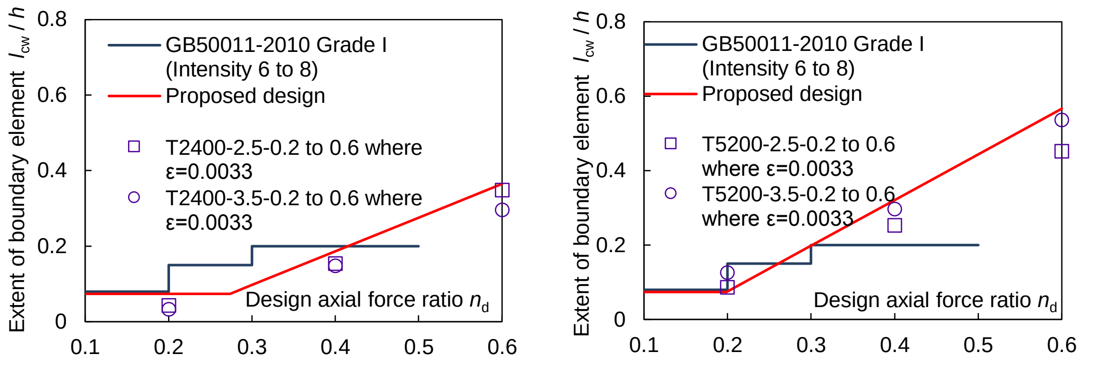


(a) T2400 (b) T5200

Fig. 15. Extent of the boundary elements at the non-flange ends of the walls.

The analysis results also indicate that for a flange in compression, the maximum compressive strains developed at the flange end are less than 0.0033 for these T-shaped walls, except for the cases of T2400-2.5-0.6 and T2400-3.5-0.6. The boundary elements at the flange ends of T2400-2.5-0.6 and T2400-3.5-0.6 are over the region where the compressive strain exceeds 0.0033. These results thus validate the effectiveness of the proposed design formulas.

Figure 16 presents the total extent of the boundary elements at two edges for the T-shaped walls. The proposed design formulas produce a longer boundary element at the non-flange end and a shorter boundary element at the flange end, when compared with the walls that were designed according to the GB50011-2010 provisions. As such, the proposed design does not require a larger total area for the boundary elements than those produced using the GB 50011-2010 provisions, but does still lead to improved performance in the T-shaped walls.

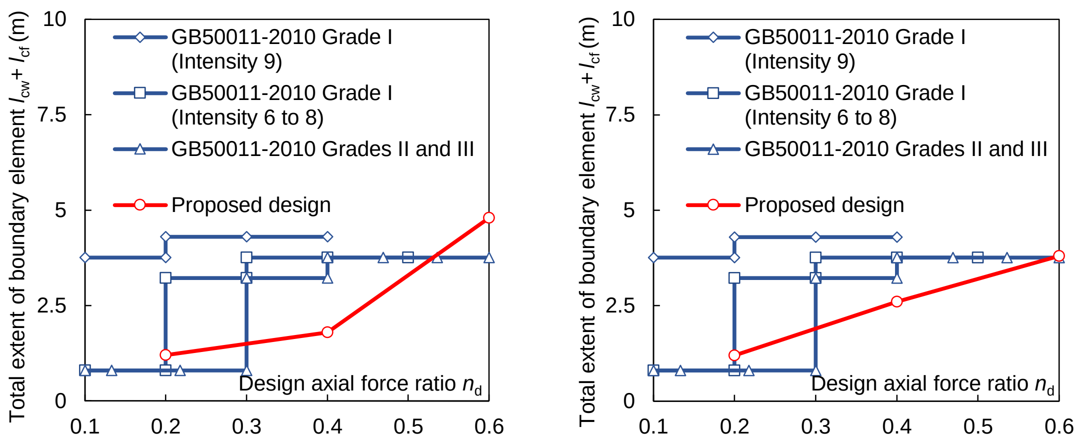


(a) T2400 (b) T5200

Fig. 16. Total extent of boundary elements at two edges for the T-shaped walls.

The numerical analysis results also indicate that, at the drift of 0.01, the maximum compressive strain that developed at the wall edges is less than the compressive strain capacity of the confined concrete in the boundary element. The compressive strain capacity of the confined concrete is defined as the post-peak strain at the instant when the compressive stress decreases to 50% of the peak stress value, and it is estimated using the empirical formulas in Mander et al. (1988).

## 6. Conclusions

This paper compares the designs of the special boundary elements for T-shaped RC walls based on the requirements of the GB 50011-2010 and ACI 318-14 codes. A displacement-based design method for the T-shaped walls is proposed, and is validated by extensive numerical analysis. The major conclusions obtained from this study are as follows:

1) The GB 50011-2010 design provisions produce shorter special boundary elements at the non-flange end when compared with the designs based on the ACI 318-14 provisions, while the former require longer boundary elements at the flange end than the latter.

2) A case study of the performance of typical T-shaped walls under high axial force ratios indicates that the boundary element at the non-flange end designed in accordance with the GB 50011-2010 provisions is insufficient, while the design of the boundary element at the flange end is overly conservative.

3) The numerical analysis indicates that the proposed displacement-based design results in improved performance for the T-shaped walls, and this improvement does not require an increase in the total area of the boundary elements at the two ends when compared with the designs based on the GB 50011-2010 provisions.

Large-scale testing on T-shaped walls will be necessary for further validation of the proposed design formulas, and this will form the subject of our future studies.

## REFERENCES

ACI (American Concrete Institute) (2014), "*Code Requirements for Structural Concrete (ACI 318-14) and Commentary*," American Concrete Institute, Farmington Hills, MI.

Brueggen BL (2009), "*Performance of T-Shaped Reinforced Concrete Structural Walls under Multi-Direction Loading*," Ph.D. thesis, University of Minnesota, Minneapolis, MN.

CEN (European Committee for Standardization) (2004), "*Eurocode 8: Design Provisions for Earthquake Resistance – Part 1: General Rules, Seismic Actions and Rules for Buildings*," European Committee for Standardization, Brussels.

Choi CS, Ha SS, Lee LH, Oh YH, and Yun HD (2004), "Evaluation of Deformation Capacity for RC T-Shaped Cantilever Walls," *Journal of Earthquake Engineering*, 8(3): 397–414.

CMC (China Ministry of Construction) (2010), "*Code for Design of Concrete Structure (GB 50010-2010)*," China Architecture & Building Press, Beijing. (in Chinese)

CMC (China Ministry of Construction) (2010), "*Code for Seismic Design of Buildings (GB*

*50011-2010)*," China Architecture & Building Press, Beijing. (in Chinese)

FEMA (Federal Emergency Management Agency) (2012), "*Seismic Performance Assessment of Buildings (FEMA P-58)*," Applied Technology Council, Redwood City, CA.

Goodsir WJ (1985), "*The Design of Coupled Frame-Wall Structures for Seismic Actions*," Doctoral dissertation, University of Canterbury, Christchurch.

LATBSDC (Los Angeles Tall Buildings Structural Design Council) (2008), "*An Alternative Procedure for Seismic Analysis and Design of Tall Buildings Located in the Los Angeles Region*," Los Angeles Tall Buildings Structural Design Council, Los Angeles, CA.

Li XL (2011), "*Mechanical Model and Test Study of High-Rise Building on Short-Leg Shear Wall Structure*," Doctoral dissertation, Xi'An University of Architecture & Technology, Xi'An.

Liang ZY (2007), "*Study on Seismic Behavior of SRC Shear Walls under High Axial Compression Ratio*," Master's Thesis, Tsinghua University, Beijing. (in Chinese)

Liu D (2014), "*Code Comparison for Seismic Design of Reinforced Concrete Walls*," Bachelor's thesis, Tsinghua University, Beijing. (in Chinese)

Lu X and Yang J (2015), "Seismic Behavior of T-Shaped Steel Reinforced Concrete Shear Walls in Tall Buildings under Cyclic Loading," *The Structural Design of Tall and Special Buildings*, 24(2): 141–157.

Mander JB, Priestley MJ, and Park R (1988), "Theoretical stress-strain model for confined concrete," *Journal of Structural Engineering*, 114(8): 1804–1826.

Moehle JP, Ghodsi T, Hooper JD, Fields DC, and Gedhada R (2011), "*Seismic Design of Cast-in-Place Concrete Special Structural Walls and Coupling Beams*," Applied Technology Council, Redwood City, CA.

Moehle J (2014), *Seismic Design of Reinforced Concrete Buildings*, McGraw-Hill Education, New York, NY.

Qian J, Cheng L, and Zhou D (2002), "Behavior of Axially Loaded Concrete Columns Confined With Ordinary Hoops," *Journal of Tsinghua University*, 42(10): 1369–1373. (in Chinese)

Thomsen IV JH, and Wallace JW (2004), "Displacement-Based Design of Slender Reinforced Concrete Structural Walls: Experimental Verification," *Journal of Structural Engineering*, 130(4): 618–630.

Wallace JW (1994), "New Methodology for Seismic Design of RC Shear Walls," *Journal of Structural Engineering*, 120(3): 863–884.

Zhang PL and Li QN (2013), "Cyclic Loading Test of T-Shaped Mid-Rise Shear Wall," *The Structural Design of Tall and Special Buildings*, 22(10): 759–769.